Modelling of the Physiological Response of the Brain to Stroke

Piotr Orlowski, David O'Neill, Vicente Grau, Yiannis Ventikos and Stephen Payne
Institute of Biomedical Engineering, Department of Engineering Science, University of Oxford, Oxford, UK

1 Introduction

Identification of salvageable brain tissue is a major challenge when planning the treatment of ischemic stroke. As the standard technique used in this context, the *perfusion-diffusion mismatch* has not shown total accuracy [1] there is an ongoing search for new imaging protocols that could better identify the region of the brain at risk [2] and for new physiological models that could on one hand incorporate the imaged parameters and predict the evolution of the condition for the individual, and on the other hand identify future biomarkers and thus suggest new directions for the design of imaging protocols. Recently, models of cellular metabolism after stroke [3] and blood brain barrier transport at tissue level [4] have been introduced. We now extend these results by developing a model of the propagation of key metabolites in the brain's extracellular space due to stroke related oedema and chemical concentration gradients between the ischemic and normal brain. We also couple the resulting chemical changes in the extracellular space with cellular metabolism. Our work enables the first patient specific simulations of stroke progression with finite volume models to be made.

2 Mathematical models

We combine a metabolism model in both neurons and astrocytes, including, among others, Na^+, Ca^{2+}, K^+, H^+, lactate, glucose, CO_2 and O_2 dynamics [3], with a model of the variation of cellular volume as a function of changing intra and extracellular ion concentrations. A model of the size and tortuosity of the brain's extracellular matrix varying as a function of cellular volume is included to allow quantification of the propagation of metabolites. Thus, the combined model results in a reaction-diffusion problem. The components of the full model are summarized in Fig. 1.

2.1 Modelling osmosis

We assume that at steady state for the model in [3] the pressure difference across the cellular membrane is 0 Pa and that for any pressure the elastic restoring force of the membrane is negligible. Further we assume that: a) any membrane pressure gradient created by lactate, glucose, CO_2 and O_2 is negligible compared to expected gradients from ionic concentrations; b) the extra- and intra-cellular space is electro-neutral; c) $[CO_3^{2-}]$ and $[H^+]$ are considered to be negligible compared to $[HCO_3^-]$; d) electro-neutrality is ensured through

$$[Na^+]_i+[K^+]_i+2[Ca^{2+}]_i-([Cl^-]_i+[HCO_3^-]_i+ z_A[A]_i) = 0, \quad (1)$$

where [A] denotes the concentration of non-permeable anions in the intra-cellular space, z_A is the magnitude of the concentration-averaged charge of the non-permeable anions and subscripts *e* and *i* indicate extra- or intra-cellular concentrations; and

$$[Na^+]_e+[K^+]_e+2[Ca^{2+}]_e-([Cl^-]_e+[HCO_3^-]_e) = 0. \quad (2)$$

$[Cl^-]_e$ is set by solving equation (2), $[Cl^-]_i$ is set based on literature [5]. It is assumed that the cellular membrane is impermeable to Cl ions. Based on previous assumptions it must be true that

$$([Na^+]_e+[K^+]_e+[Ca^{2+}]_e+[Cl^-]_e+[HCO_3^-]_e) - ([Na^+]_i+[K^+]_i+[Ca^{2+}]_i+[Cl^-]_i+[HCO_3^-]_i+[A]_i) = 0, \quad (3)$$

and it is thus possible to determine z_A and $[A]_i$. Ion concentrations further depend on diffusion.

2.2 Modelling of diffusion in the extracellular matrix

The diffusion of molecules in the brain's extracellular space is modelled according to Fick's Law. Thus, the rate of change of a substrate concentration [S] can be written as

$$\frac{\partial[S]}{\partial t} = \frac{D_s}{\lambda^2}\nabla^2[S] + \frac{q}{\alpha}, \quad (4)$$

where D_s is the diffusion coefficient of substrate *S*, q is the rate of change of substrate concentration due to chemical reactions, α is the proportion of extracellular space in the volume and λ is the space's tortuosity. Diffusion coefficients for key metabolites are readily available in literature [5-9] for 300K and at infinite dilution. Values were adjusted to the human body temperature of 310K using the relationship in [10]. In the case of lactate the diffusion coefficient was estimated using Einstein's formula as reported in [11]. Infinite dilution was assumed for all species. The numerical values of α

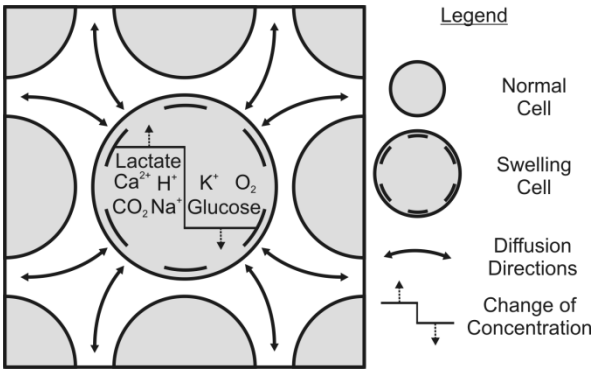

Figure 1. Schematic representation of cell membrane depolarization and associated swelling and diffusion of molecules in the extracellular space.

Molecule	Diffusion [10^{-5}xcm^2.s^{-1}]	Source
Na^+	1.37	[6]
Ca^{2+}	0.82	[6]
K^+	2.02	[6]
Cl^-	2.10	[6]
H^+	9.62	[6]
Lactate	1.1	[11]
Glucose	0.67	[9]
CO_2	2.80	[7]
O_2	2.98	[8]
Parameter	Range of Values	Source
α	0.12-0.31	[12]
λ	1.39-1.95	[12]

Table 1. List of parameters affecting diffusion of ions and metabolites in the extracellular space including brain's porosity and tortuosity.

and λ can be estimated by monitoring the evolution of the concentration of an injected impermeable ion in the brain space [12]. The brain is fairly homogenous regarding these parameters: mode values of α and λ emerging from the analysis of a range of brain regions and species are 0.2 and 1.6 respectively, with extreme reported values for α being 0.12 and 0.31 [12]. The anisotropy of the tortuosity in the brain space has been investigated, leading to estimates ranging from 1.39 to 1.95 depending on the direction. The directionality is mostly pronounced in the white matter.

The model in section 2.1 allows the simulation of the growth of cells resulting from the osmotic stress following the depolarization of the cellular membrane during severe ischemia. Thus, in our model α is time dependent as the proportion of space occupied by astrocytes and neurons changes. The study in [13] showed that λ remains constant during osmotic challenge. However, this conclusion was made based on the analysis of a 2D matrix only. Using a geological analogy a relationship between λ and α was proposed in [14]:

$$\lambda^2 = \alpha^{-\beta} \tag{5}$$

where β usually lies between 1/2 and 2/3. However, as this expression is a power law, accurate testing of its validity would require the changing of parameters over at least an order of magnitude which is not possible for the brain. We set β by solving equation (5) for λ=1.6 and α is set based on [3]. With α being a function of time and space the combination of equations (4) and (5) leads to

$$\frac{\partial \alpha[S]}{\partial t} = D_s \nabla^2 \alpha^{1+\beta}[S] + q. \tag{6}$$

2.3 Full model mathematical formulation

Based on [3] and the previous sections the whole model can be summarized by a system of equations assuming that the change of the total mass of reactants in a finite volume of the brain is due to either diffusion, changes in blood supply or chemical reactions. Thus, we can write

$$\mathbf{M}\dot{\mathbf{u}} = \mathbf{F}_{\text{diff}}(\mathbf{u}) + \mathbf{F}_{\text{blood}}(\mathbf{u}) + \mathbf{F}_{\text{chem}}(\mathbf{u}), \tag{7}$$

Where $\mathbf{M}$ is a mass matrix for a vector of temporal derivatives $\dot{\mathbf{u}}$, while $\mathbf{F}_{\text{diff}}(\mathbf{u})$, $\mathbf{F}_{\text{blood}}(\mathbf{u})$ and $\mathbf{F}_{\text{chem}}(\mathbf{u})$ are respectively diffusion, blood flow and chemical reactions forcing functions.

3 Implementation

OpenCell (University of Auckland, Auckland NZ) software was used for the design and testing of the model at the cellular level and to make its fundamental Fortran implementation available for further development and computation. CellML code from [3] was used as the development base for the model. CFD-VISCART (ESI-Group, Paris, France) was used for meshing the 3D model of the brain extracted from imaging data. Matlab and Fortran were used for the mapping of post stroke perfusion levels on mesh cells. The CFD-ACE (ESI-Group, France) finite element solver was used for the coupled PDE-ODE problem with the FCVODE library (Sundials, University of California, USA) to compute simultaneous ODEs.

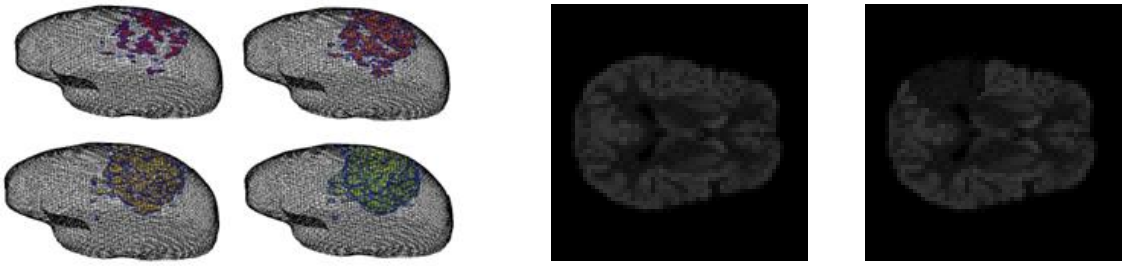

Figure 2. Left: 3D model of the brain. Isosurfaces represent CO_2 concentration after stroke. Darker colours refer to higher values. Right: Pre- and post-stroke synthetic images for model computational testing

4 Results

We used synthetic images of Cerebral Blood Flow (CBF) of a fictitious post-stroke patient (Fig.2) created based on full head Arterial Spin Labelling (ASL) perfusion images of a healthy individual to construct a 3D finite volume model of the brain. For a ~50 000 voxel brain volume, ~150 000 mesh cells were created. A plane of symmetry cutting the brain into an ischemic half and an unaffected half was found. Percentage change of CBF per voxel of the ischemic half was defined as the ratio of the intensity of the voxel to the corresponding symmetric voxel intensity. The model in [3] governed metabolism in each of the mesh cells and was personalised with calculated CBF changes. Fig. 2 presents simulated changes in the concentration of CO_2 concentration in the brain after stroke. The currently un-optimised code required 4 minutes computation per second simulation step.

5 Discussions

We introduced a novel method for the simulation of stroke progression in 3D that can be personalised with quantitative perfusion imaging. For real-time simulation, a speed improvement of the order of three orders of magnitude will be required. The cerebrospinal fluid (CSF) moves in the brain at a speed of ~10 μm/min and diffusion is only between one and two orders of magnitude faster. This means that CSF dynamics models similar to those in [15] may have to be added. Similarly a model of the movement of ions in electrolyte solutions will be added. We are currently gathering post-stroke perfusion and tractography data to test the model with clinical images and model tissue anisotropy.

6 Acknowledgements

This work was supported by the Centre of Excellence in Personalised Healthcare funded by the Wellcome Trust and EPSRC under grant number WT 088877/Z/09/Z.

7 References

[1] Kidwell CS, Alger JR, Saver JL. Beyond Mismatch: Evolving Paradigms in Imaging the ischemic Penumbra with multimodal magnetic resonance imaging. *Stroke*, 34: 2729-2735, 2003.

[2] Zhou J, Payen JF, Wilson DA, Traystman and van Zijl. Using the amide proton signals of intracellular proteins and peptides to detect pH effects in MRI. *Nature Med* 9(8):1085-1090, 2003.

[3] Orlowski P, Chappell M, Sub Park C, Grau V and Payne S. Modelling of pH dynamics in brain cells after stroke. *Interface Focus* 1:408-416, 2011.

[4] Su SW, Catherall M and Payne S. The influence of Network Structure on the Transport of Blood in the Human Cerebral Microvasculature. *Microcirculation*, 19(2):175-187, 2012.

[5] Harned HS, Owen BB. The Physical Chemistry of Electrolytic Solutions, Reinhold, New York, 1958.

[6] Robinson RA, Stokes RH, Electrolyte Solutions, Butterworths, London, 1965.

[7] B. Jähne, G. Heinz and W Dietrich. Measurement of the Diffusion Coefficients of Sparingly soluble Gases in Water. *Journ*al of Geophysical Research 92:767-776, 1987.

[8] CE St.-Denis and CJD Fell. Diffusivity of oxygen in water. *Can. J. Chem. Eng.* 49:885, 1971.

[9] Longsworth LG, Diffusion Measurements, at 25°, of Aqueous Solutions of Amino Acids, Peptides and Sugars, J. Am. Chem. Soc., 75, 5705, 1953.

[10] Bastug T and Kuyucak S. Temperature dependence of the transport coefficients of ions from molecular dynamics simulations. Chemical Physics Letters 408:84-88, 2005.

[11] Pfeuffer J, Tkac I, Gruetter R. Extracellular-Intracellular Distribution of Glucose and Lactate in the Rat Brain Assessed noninvasively by Diffusion-Weighted ^{1}H Nuclear Magnetic Resonance Spectroscopy *In Vivo*. *J. Celeb. Blood Flow Metab.* 20:736-746, 2000.

[12] Nicholson C. Diffusion and related transport mechanisms in brain tissue. *Rep. Prog. Phys.* 64:815-884, 2001.

[13] Chen KC and Nickolson C. Changes in brain cell shape create residual extracellular space volume and explain tortuosity behaviour during osmotic challenge. *Proc. Natl. Acad. Sci. USA* 97:8306-8311, 2000.

[14] Nickolson C and Rice ME. The migration of substances in the neuronal microenvironment. *Ann. NY Acad. Sci.* 481:55-71, 1986.

[15] Tully B and Ventikos Y. Cerebral water transport using multiple-network poroelastic theory: application to normal pressure hydrocephalus. *Journal of Fluid Mechanics* 667:188-215, 2011.